JETIR.ORG ISSN: 2349-5162 | ESTD Year : 2014 | Monthly Issue
JOURNAL OF EMERGING TECHNOLOGIES AND INNOVATIVE RESEARCH (JETIR)
An International Scholarly Open Access, Peer-reviewed, Refereed Journal

Influence of Sn dopants on the response of zinc oxide (ZnO) thin films to acetone vapour

Rajarshi Krishna Nath

Department of Physics, Gurucharan College, Silchar, Cachar, Assam, India.

Abstract: A spray pyrolysis technique have been used to fabricate Sn-doped zinc oxide (ZnO:Sn) thin films using Zn $(CH_3COO)_2$ as a precursor solution and $SnCl_4$ as the doping solution. The concentration of doping is varied from 0 to 1.5 at%. The structural, morphological, optical and electrical properties of the films are explored and then tested for acetone sensing. Structural studies show that the films are polycrystalline in nature, possessing "hexagonal wurtzite" structure. The optical energy gap is found to be increasing with an increase in Sn doping concentration. The resistivity of the films decreases with dopant concentration up to 0.5at%, while at a higher doping concentration of 1at%, the disorder produce in the lattice causes an increase in the resistivity of the film. It is observed that compared to undoped ZnO film, ZnO:Sn films show higher response to acetone. Among all the doped films studied, the 0.5 at% Sn doped ZnO film show the highest response (92.03%) to 500 ppm of acetone in air at 300^0C. Further the films show faster response and recovery at higher operating temperatures.

Key words: ZnO:Sn thin film, spray pyrolysis, acetone vapour.

1.Introduction

The use of solid- state gas sensor has been increasing at an outstanding rate for the last few decades due to its use as the chemical sensitivity of semiconductor surfaces to different adsorbed gases. Presence of dopant elements to an appropriate amount can produce various electronic defects, which increase the influence of oxygen partial pressure on the resistivity. Zinc oxide (ZnO) is an important metal-oxide semiconductor for sensing toxic pollutant gases, combustible gases and organic vapours. Doped ZnO thin films have numerous attractive applications in electronic and optoelectronic devices such as transparent electrodes, solar cell windows, piezoelectric devices, gas sensors etc. For gas sensing purposes, this material has been investigated in

various forms such as single crystals, sintered pellets, thick films, thin films as well as heterojunctions. [1-5]. However, thin films are more suitable for gas sensing purposes, as the gases are adsorbed on the material surface and the surface reactions occur. This reaction modifies the concentration of charge carrier in the material, giving rise to a change in its electrical property such as resistance/conductance.

Various methods for the synthesis of thin films have been developed by several researchers for gas sensing applications. These include chemical vapor deposition, sol-gel process, spray pyrolysis, sputtering etc. Paraguay et al studied the influence of Al, In, Cu, Fe and Sn dopants on the response of thin film ZnO gas sensor to ethanol vapour. [6]. Sahay et al had studied Al-doped zinc oxide thin films for liquid petroleum gas (LPG) sensors. [7]. T.Minami. et al have investigated Group III impurity doped zinc oxide thin films prepared by RF magnetron sputtering[8]. In this work, we have investigated the structural, morphological, optical and electrical properties Sn-doped zinc oxide (ZnO:Sn) thin films prepared by spray pyrolysis technique and finally the sensing behavior of these films towards acetone vapour is studied, as exposure of acetone vapor to human beings is harmful.

2. Experimental

The glass substrates (microscopic slides) prepared in 37.5 mm× 12.5mm × 1.35 mm dimensions are subsequently cleaned in freshly prepared chromic acids, followed by detergent solution and distilled water. The cleaned substrates are placed on hot plate at a constant temperature of $(410 \pm 10)^0$ C. The precursor solution used is of 0.1M concentration of high purity zinc acetate dehydrate (Merck, India) prepared in distilled water. The compound sources of dopants are aluminium chloride. The atomic percentage of dopants in the solution is varied from 0 to 1.5 at%. The atomization of the solution into a spray of fine droplets is carried out by the spray nozzle, with the help of a compressed air as carrier gas. A schematic representation of the typical spray pyrolysis setup, developed in our laboratory and various process parameters for the deposition of films is reported elsewhere [9]. The substrate temperature is monitored using a chromel-alumel thermocouple with the help of a Motwane digital multimeter (Model: 454). During optimization of the process parameters, the substrate temperature has been found to be the most important parameter in film preparation for gas sensing applications. The thickness of the films is measured by the weight difference method using an electronic high precision balance (Citizen, Model: CY 204) & are found to lie within 200-300nm with an error of ±10%.

. Structural analysis of the films is carried out using a PANalytical X'Pert Pro X-ray diffractometer with CuKα radiation (λ = 1.5418 Å) as an X-ray source at 40kV and 30mA in the scanning angle (2θ) from 30 to 70^0 with a scan speed 0.02^0/ s. The optical transmission spectra of the films are obtained in the UV/ VIS/ near IR region up to 1100 nm using Perkin Elmer UV-VIS spectrophotometer (Model: Lamda 35). The morphological studies are carried out using Transmission Electron Microscope (Model: JEM 1000C X II). High conducting silver paste is used to make ohmic contacts on both the ends of the films and is dried at a temperature of 150^0C. The film is mounted on a home made two-probe assembly placed into a silica tube, which is inserted coaxially inside a tubular furnace. The electrical resistance of the film is measured before and after exposure to acetone vapour using a Keithley System electrometer (Model: 6514). The sensing characteristics of the film under different concentration levels of acetone are studied at different operating temperature in the range 225^0C–350^0C. To study sensing properties of the film required volume of acetone is injected into the closed silica tube maintained at various temperatures, and subsequently, the decrease in film resistance is monitored till it becomes stationary. Finally, both ends of the tube are opened and the film resistance is allowed to recover the initial value in air.

3. Results and discussion

3.1. Structural analysis

Fig. 1 shows the X-ray diffraction patterns of the typical Sn-doped ZnO films.

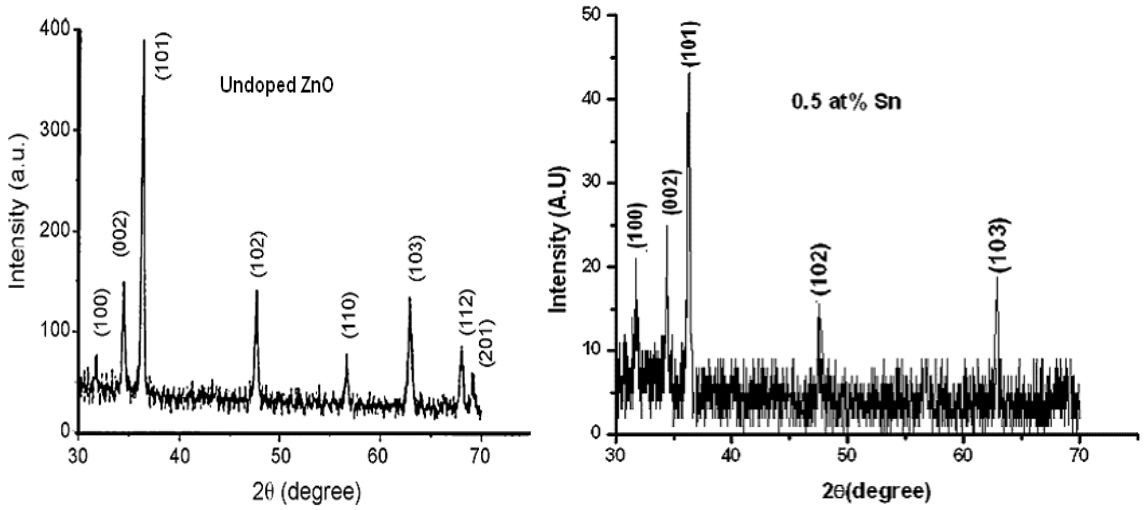

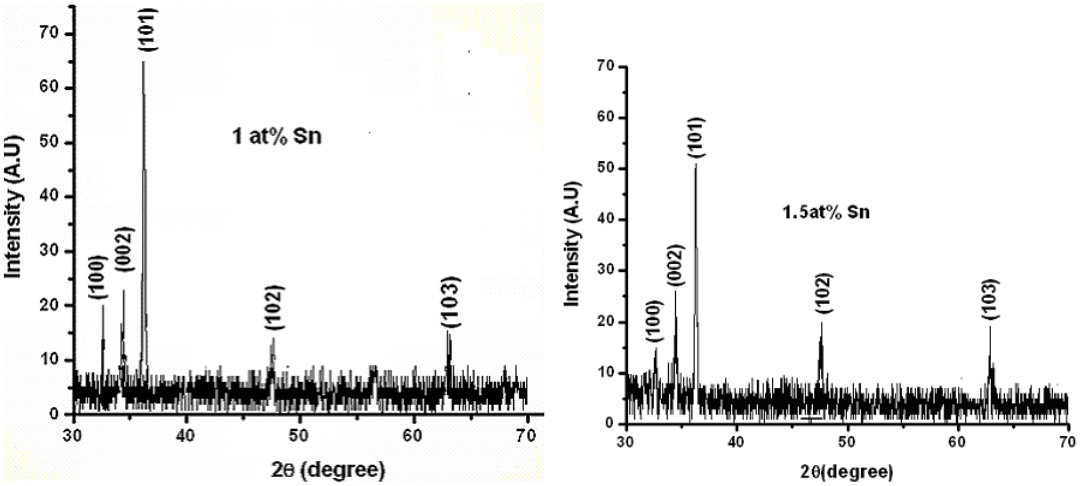

Fig.1. XRD patterns of the typical Sn-doped ZnO thin films

All the films are found to be polycrystalline in nature, possessing "hexagonal wurzite" structure as per ICDD reference pattern (01-070-8070). No phase corresponding to tin or other tin compound is observed in the XRD patterns, which indicates a low level incorporation of tin in ZnO film.[20] All the Sn-doped ZnO films show the most intense peak corresponding to (101) plane while the other planes corresponding to (100), (002), (102), (103), etc, are present with low relative intensities. The crystallite size of the films is calculated using Debye-Scherrer equation.

$$D = \frac{0.9\lambda}{W Cos\theta} \quad \text{---------- (1)}$$

It is observed that the crystallite size of 0.5at% Sn-doped ZnO film is less than that of undoped ZnO of similar thickness. This is due to the lesser ionic radius of Sn^{+4} (R_{Sn}^{+4} = 0.071 nm) which substitutes Zn^{+2} (R_{Zn}^{2+} = 0.074 nm), thereby decreasing the crystallite size. However, crystallite size does not vary systematically with Sn dopant concentration, which is attributed to the lattice disorder produced in the films at higher dopant concentrations due to the difference in their ionic radii.[17]

3.2. Morphological studies

The TEM images of Sn-doped ZnO samples are displayed below.

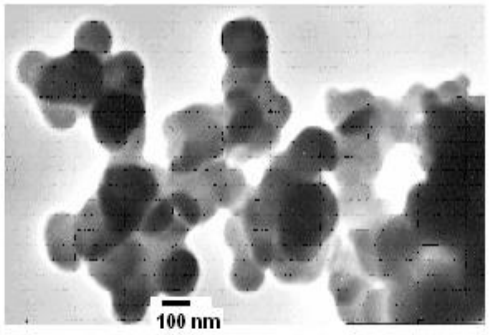

Undoped ZnO

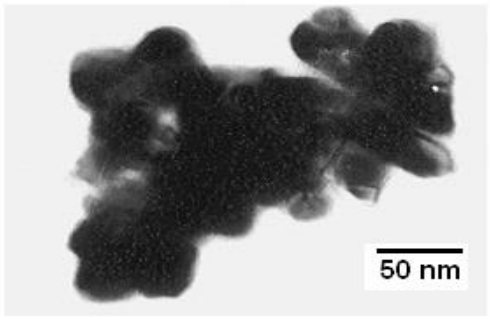

0.5at% Sn-doped ZnO

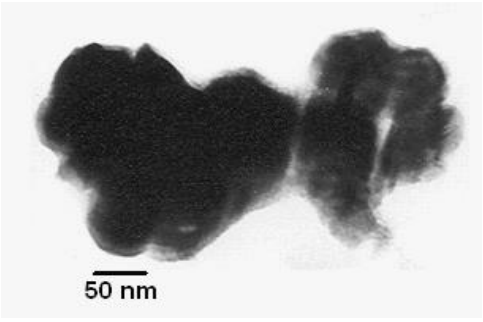

1 at % Sn-doped ZnO

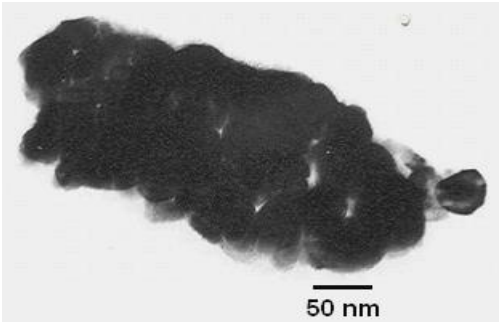

1.5 at% Sn-doped ZnO

Fig.2. TEM images of Sn-doped ZnO samples

The crystallite sizes of ZnO:Sn samples obtained from TEM & XRD are given in table 1.

Samples	Crystallite size (nm) (From TEM)	Crystallite size (nm) (From XRD)
Undoped ZnO	149.8	156 ±1.23
0.5 at % ZnO:Sn	41.7	47± 0.45
1 at % ZnO:Sn	67.8	74 ± 0.79
1.5 at % ZnO:Sn	58.2	65± 0.65

Table.1.Crystallite size of Sn-doped ZnO samples from TEM & XRD studies

3.3 Optical studies

Figure 3 shows the optical transmission spectra of zinc oxide films prepared at substrate temperature of 410 ± 10^0C for different Sn doping concentrations (0 to 1.5at %).

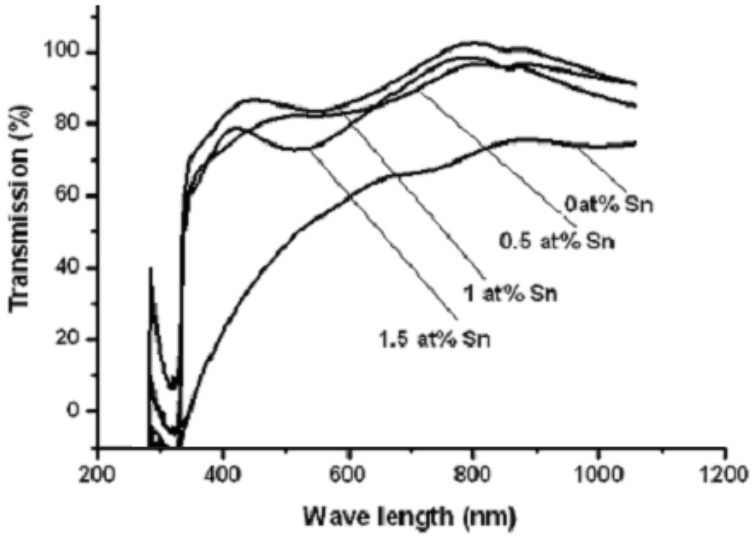

Fig.3. Transmission spectra of undoped and Sn-doped ZnO thin films.

These spectra reveals that in all the doped films, the average transmission over the range 400- 1100 nm is more than 80% with a sharp fall near the fundamental absorption, whereas fall in transmission is gradual in undoped ZnO film. The ripples observed in these spectra are due to the interference fringes arising from the substrate-film and film-air interfaces.[19] These fringes smoothen out as the doping concentration decreases

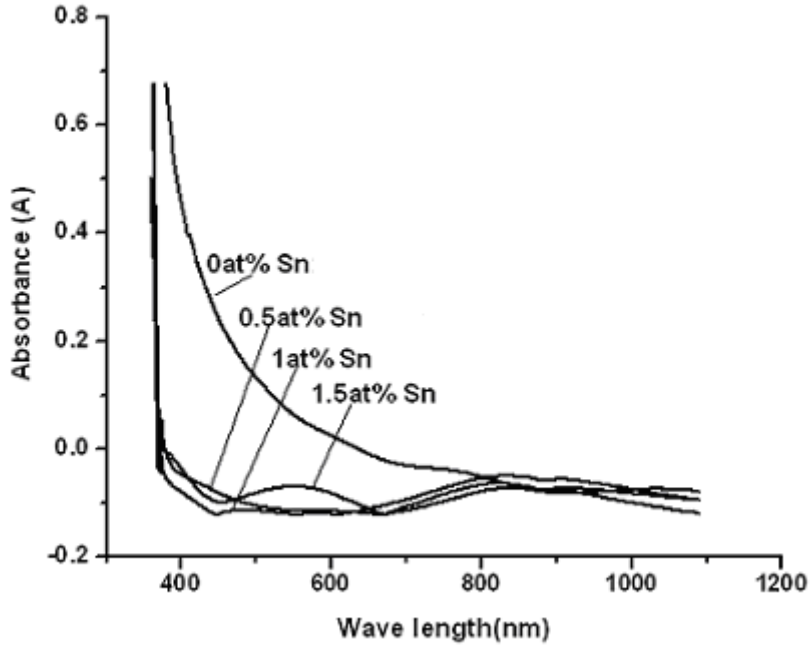

Fig.4. Absorbance spectra of undoped and Sn-doped ZnO thin films

The optical absorption spectra of the ZnO:Sn films with different Sn dopant concentration (0 to 1.5 at %) as a function of wavelength are shown in figure 4. It is evident from the figure that the films grown under the same process parameter have low absorbance in the visible/near infrared region while the absorbance is high in the ultraviolet region. Further a steep rise in the absorbance near the absorption edge is observed for all the doped films that hint at a direct type transition.

The absorption coefficient (α) is calculated using Lambert law as follows [19]

$$\mathrm{Ln}\left[\frac{I_o}{I}\right] = 2.303\,A = \alpha\, d \quad \text{----------} \quad (2)$$

where I_o and I are the intensity of incident and transmitted light respectively, A is the optical absorbance and d the film thickness.

The absorption coefficient (α) was found to follow the relation----

$$\alpha = \frac{[\,A\,(hv - E_g)^{1/2}\,]}{hv} \quad \text{----------} \quad (3)$$

Where A is a constant and E_g is the optical band gap.

Plots of $(\alpha hv)^2$ versus photon energy (hv) in the absorption region near the fundamental absorption edge is shown in fig.4. In this case n = 2 gives the best linear graph which indicates direct allowed transition in the film material.

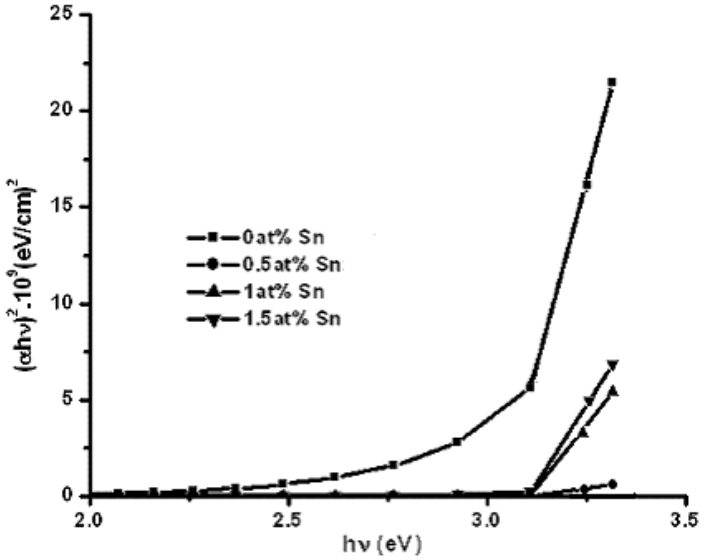

Fig.5. Plots of $(\alpha h\nu)^2$ vs hν for different Sn-doped ZnO thin films.

The optical band gap, estimated by the extrapolation of the linear region of the graph to the photon energy axis is found to be increasing from 3.02 eV to 3.13 eV with Tin (Sn) dopant concentrations from 0 to 1.5 at%. The change in band gap can be attributed due to the Burstein-Moss band gap widening and band gap narrowing due to electron-electron and electron-impurity scattering.[20]

The variation of band gap with Sn doping concentration is listed in table 2.

Film examined	Optical band gap (eV)
0 at% Sn-doped ZnO	3.02 ± 0.01
O.5 at% Sn-doped ZnO	3.09 ± 0.01
1 at% Sn-doped ZnO	3.11 ± 0.01
1.5at% Sn-doped ZnO	3.13 ± 0.01

3.4. Resistivity studies

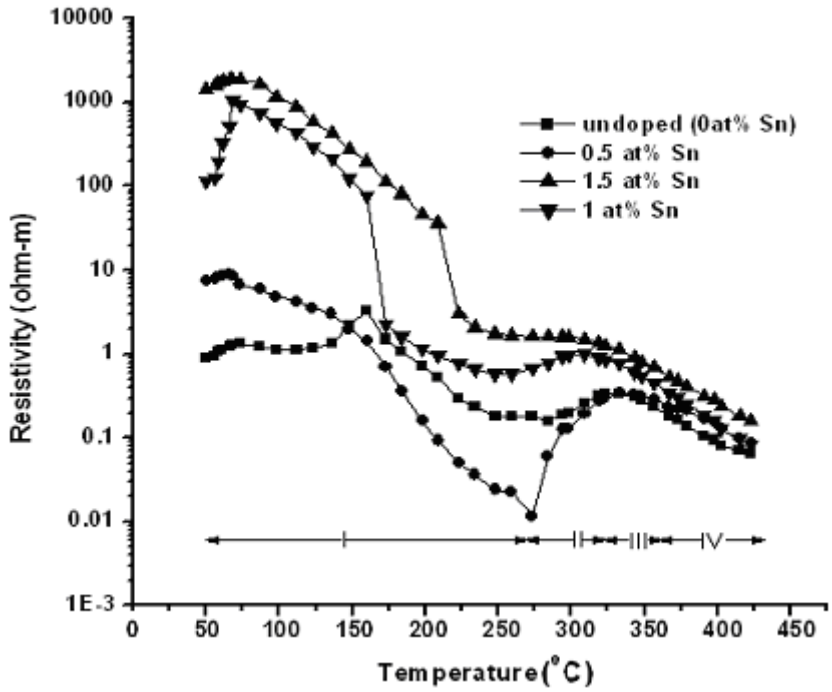

Fig.6. Variation in resistivity of undoped and doped ZnO films.

The resistivity of ZnO thin films for different Tin doping concentrations (0 to 1.5 at %) as a function of temperature is represented in figure 6. The rate of heating is 5 ^{0} Kelvin per minute. It is observed in the figure that the resistivity of all the films increases initially at the lower temperature region. This increase in resisitivity is attributed to the chemisorption of oxygen on the film surface, causing a decrease in carrier concentration. This is consistent with the adsorption of oxygen on the surface of polycrystalline ZnO films as reported by other researchers.[21] Further the resistivity of the film is found to be decreased with a small amount (0.5at %) of Sn dopant. This could be due to the replacement of Zn^{2+} by Sn^{4+} ions, which increases electron concentration, thereby decreasing the resistivity. With an increase in Sn dopant above 0.5at%, the resistivity is found to be increasing significantly. This may be due to the formation of nonconductive tin oxide from the tin atoms and the achievement of equilibrium between the tin atoms contributing conduction electrons and those producing tin oxide. Further, at higher doping concentrations, the disorder produced in the lattice (due to the difference in ionic radii of Zn^{2+} and Sn^{4+}) increases the efficiency of scattering mechanism such as phonon scattering and ionized impurity scattering which, in turn, causes an increase in resistivity.

As evident from the figure 6, the resistivity of all the films show a slight increase at lower temperatures afterwards follow the four-region behaviour (1) thermal excitation of electron ; (II) adsorption of

oxygen species; (III) equilibrium; and (IV) desorption of oxygen species; similar to that reported by Paraguay et al[6] and Sahay et al.[7].

3.5. Acetone sensing properties

The sensing characteristic of ZnO film as a function of the operating temperature for three different concentrations (100, 300, and 500 ppm) of acetone in air is shown in fig.7. It is observed that the sensitivity of the all the films increases with an increase in acetone concentration in air. The optimum operating temperature is observed to be 300^0 C in all the cases. A maximum sensitivity of 37.82% is observed to 500 ppm of acetone at 300^0C. The response of the film is determined by

$$S = \frac{(R_a - R_g)}{R_a} \times 100\ \% \text{ --------(4)}$$

where R_a = resistance of the film in air,

R_g = resistance of the film upon exposure to gas/vapor.

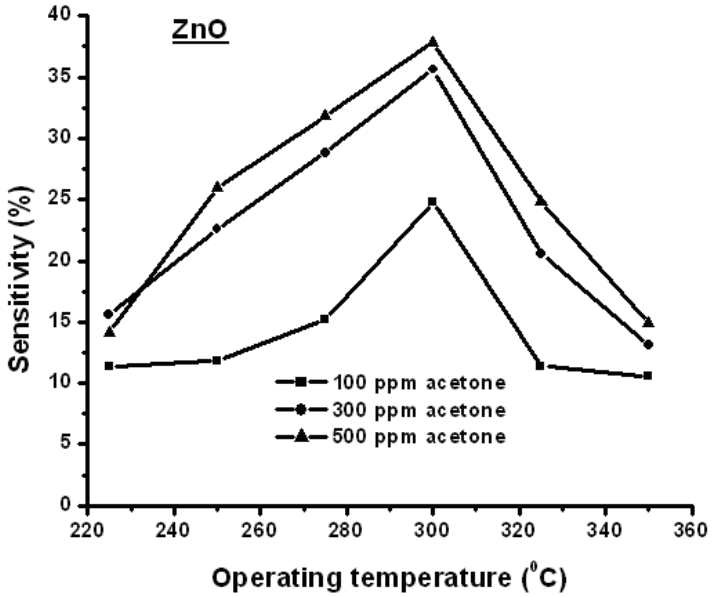

Fig.7. Variation of sensitivity of ZnO film with operating temperature for various concentration (100,300,500 ppm) of acetone in air.

3.5.1. Influence of Sn Dopant

The sensing characteristics of Sn-doped ZnO films as a function of operating temperature for three different concentrations (100, 300, and 500 ppm) of acetone in air is represented in fig.8.

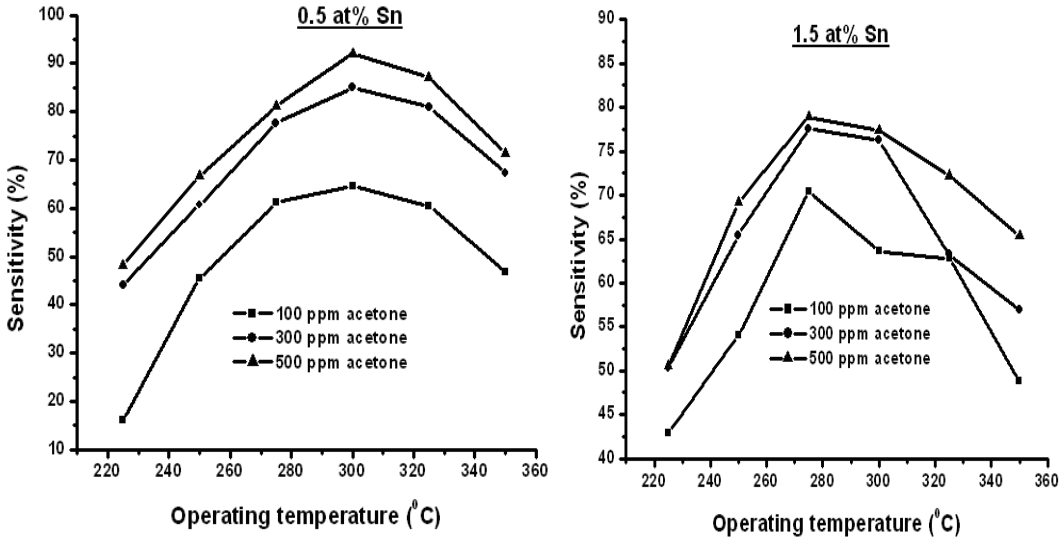

Fig.8. Sensitivity characteristics of Sn-doped ZnO films as a function of operating temperature for three different concentrations (100, 300 and 500ppm) of acetone in air.

It is observed that compared to undoped ZnO film, Sn-dopant significantly increases the sensitivity of the film towards acetone vapour. A maximum sensitivity of 92.03% is observed in case of 0.5 at% Sn-doped ZnO film to 500 ppm of acetone at 300^0 C.

This may be due to an increase in electron concentration resulting from the replacement of Zn^{2+} by Sn^{4+} as evident from the resistivity measurement. Further the response of the films to higher concentrations of acetone is found to be decreasing with increase in doping concentration. This may be due to the formation of a non-conducting tin oxide from the extra Sn atoms and the achievement of equilibrium between the Sn atoms contributing conduction electrons and those producing tin oxide, which results to an increase in the potential barrier to charge transport, thereby decreasing the sensitivity.

In general, there exists an optimum working temperature of a sensor to achieve the maximum sensitivity to a gas/vapor of interest, the temperature being dependent upon the kind of gases/vapors,i,e the mechanism of dissociation and further chemisorption of a gas/vapor on the particular sensor surface. In this work, all most all the films (undoped and doped) shows a maximum response at around “573 K” for all concentrations of acetone in air, which is therefore considered to be the optimum temperature as mentioned earlier. This is attributed to

the availability of sufficient adsorbed ionic species of oxygen on the film surface, which react most effectively with acetone molecules at this particular temperature.

At lower operating temperature, the response of the films to acetone is restricted by the speed of the chemical reaction because the gas molecules do not have sufficient thermal energy to react with the adsorbed oxygen species. Further during adsorption of atmospheric oxygen on the film surface, a potential barrier to charge transport is developed. At higher operating temperatures the thermal energy obtained is high enough to overcome the potential barrier and thus the electron concentration increases significantly due to sensing reaction, which results to an increase in response of the films.

The sensing mechanism of the film to acetone may be explained as follows. At first oxygen is adsorbed on the film surface when the film is heated in air. The adsorption of oxygen forms ionic species such as O^{2-}, O_2^- and O^- which have acquired electrons from the conduction band and desorbs from the surface at 353 K, 403 K and 773 K respectively. So in the temperature range used in this work, only O^- species, which are the most stable ones, will react with the acetone. The reaction kinematics will proceed like this. [10]

$$O_2\,(gas) \quad <=> \quad O_2\,(absorbed)$$

$$O_2\,(absorbed) + e^- \quad <=> \quad O_2^-$$

$$O_2^- + e^- \quad <=> \quad 2O^-$$

The reaction between acetone and ionic oxygen species may take place by two different ways having different rate constants (k) depending upon the temperature. [10]

$$CH_3COCH_3\,(gas) + O^- \rightarrow CH_3COCH_2 + OH^- + e^- \; ; \; k = 1.0 \times 10^{12}\; e^{(-21000/RT)}\; [cm^3/mol\ s]$$

$$CH_3COCH_3\,(gas) + OH^- \rightarrow CH_3CHO + CH_3O^- \; ; \; k = 2.0 \times 10^{12}\; e^{(-63000/RT)}\; [cm^3/mol\ s]$$

$$CH_3CHO + O\,(bulk) \rightarrow CH_3COOH + O\,(vacancies)$$

$$CH_3COCH_3\,(gas) + O^- \rightarrow CH_3CO + CH_3O^- + e^- \; ; \; k = 1.0 \times 10^{12}\; e^{(-42000/RT)}\; [cm^3/mol\ s]$$

$CH_3CO \rightarrow CH_3 + \quad CO \quad ; \quad k = 2.0 \times 10^{11} \; e^{(-15000/RT)}$ [1/ s]

$CO + O^{-} \rightarrow \quad CO_2 \quad + \; e^{-}$

From figure 8, it is clear that addition of small amounts Tin enhance the sensing behavior of the film. This increase in sensitivity for acetone vapor with the addition of Sn may be attributed to the rule tin as a dopant, which is providing additional oxygen sites.

Fig.9 represents the sensing characteristics of the two films, namely undoped ZnO, and 0.5at% Sn doped ZnO as a function of acetone concentration in air at 573 K..

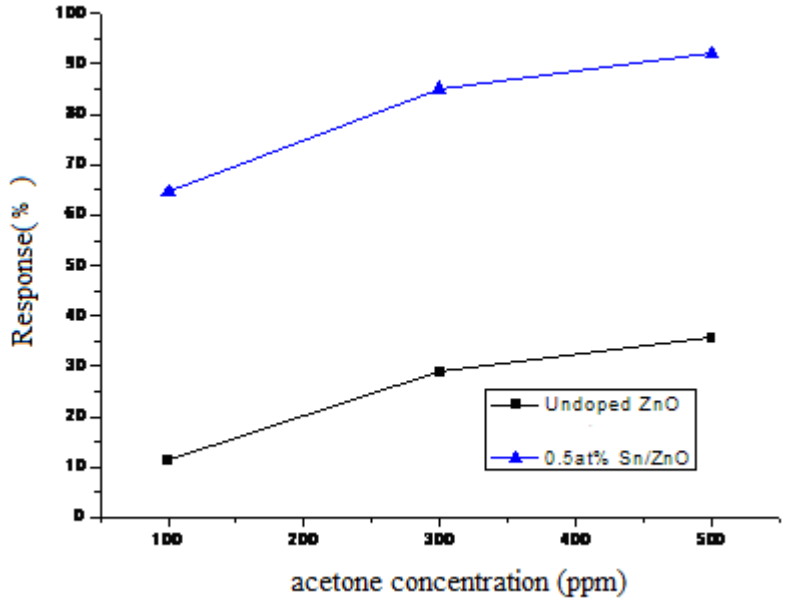

Fig.9 Sensing characteristics as a function of acetone concentration in air at 573 K for three different samples,viz, undoped ZnO, 0.5at% Al/ZnO and 0.5at% Sn/ZnO

It is evident from the figure that the sensitivity of Sn/ZnO is much greater as compared to that of undoped ZnO film, which clearly signifies the influence of Sn dopants on the response of ZnO thin film to acetone vapor. It is observed from the figure that the response increases rapidly in the lower concentration region of acetone, while it increases gradually in the higher concentration of acetone. For example for a particular film say 0.5at% Sn/ZnO, the response increases from 64.61% to 85.07% as the concentration of acetone increases from 100 ppm to 300 ppm and then increases to 92.03% when the concentration is further increased to 500 ppm. This can be attributed due to the fact for a low concentration (100 ppm), there is a smaller surface coverage of acetone molecules on the film and hence the surface reaction proceeds slowly. On an increase in concentration to 300

ppm, the surface reaction increases due to a larger surface coverage of acetone molecules, which results to a rapid increase in response. On a further increase in concentration to 500 ppm, the surface coverage of acetone molecules begins to attain saturation, which results to a gradual increase in response

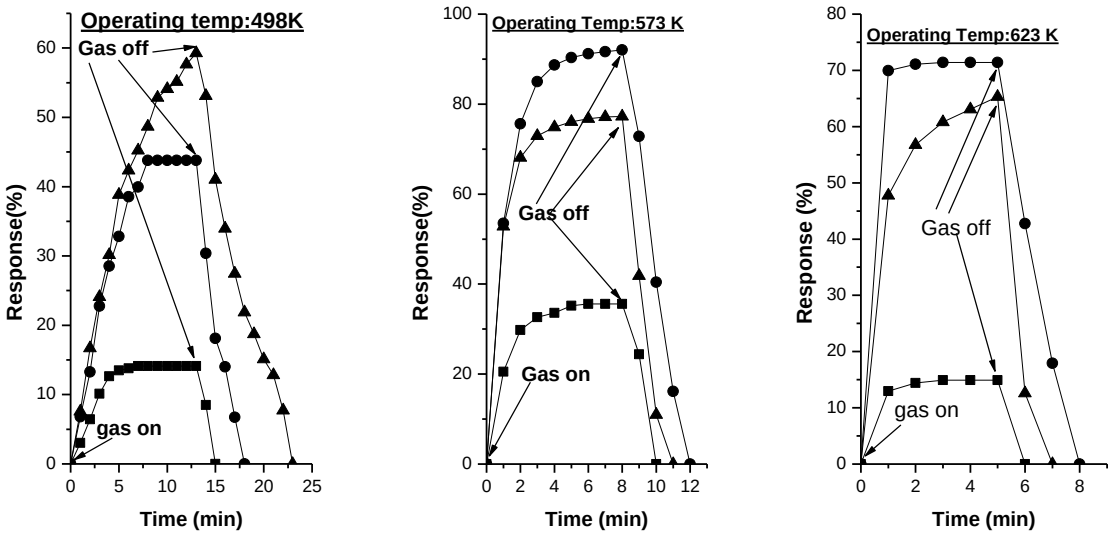

Fig.10.Transient response characteristics of (■) undoped ZnO, (▲) 0.5 at% Sn/ZnO and (●) 1 at% Sn/ZnO film to 500 ppm acetone at operating temperatures of 225ºC, 300 ºC and 350 ºC.

Fig.10 represents the transient response characteristics of the three films, viz undoped ZnO, 0.5 at% Sn/ZnO and 1at% Sn/ZnO towards 500 ppm of acetone at three different operating temperatures (225ºC, 300 ºC and 350 ºC). It is observed in the figure that al the three samples show fast response and recovery to acetone at higher operating temperatures. This is basically due to the fact at higher operating temperature, the surface reaction becomes faster due to sufficient thermal energy. Also, at each operating temperature, the undoped film shows faster response as well as recovery to acetone in comparison with the other two doped films. In this work, the average response time and recovery time for all the doped films were found to be respectively 7 min and 3 min.

4. Conclusion.

Undoped, and Tin doped zinc oxide thin films prepared by chemical spray pyrolysis technique have been studied for acetone sensors. The UV/VIS spectra of the films reveal that the films show a direct electronic transition with an energy gap of 3.27 eV. The resistivity of the films prepared under same parametric conditions are found to vary with the dopant elements and a typical four region behavior of resistivity with temperature is seen for all the films.

The acetone sensing characteristics of the films are found to be highly influenced by the presence of dopant elements. It is observed that the doped films show more than double response to acetone vapor as

compared to that of undoped ZnO film. Among all the films studied, the 0.5 at% Sn doped ZnO film shows the maximum response (92.03%) at 300ºC to 500 ppm of acetone in air, whereas in the case of undoped ZnO, the response is found to be 35.61% at the same operating temperature and same concentration of acetone in air. The films show fast response and recovery to acetone at higher operating temperatures.

Acknowledgement

The authors wish to acknowledge Dr. P.P.Sahay**,** Department of Physics, MNNIT, Allahabad, UP, India for his technical assistance in this work.

References

[1] J.A. Anna Selvan, H. Keppner, A. Shah, The grouth of surface textured aluminium doped ZnO films for a Si:H solar cells by RF magnetron sputtering at low temperature, Mater. Res. Soc. Symp. Proc. 426 (1996) 497-502.

[2] K.L Chopra, S. Major, D. R. Pandya, Transparent conductors-a status review, Thin Solid Films 102 (1983) 1-46

[3} V. Gupta, A. Mansingh,, Influence of post deposition annealing on the structural and optical properties of sputters zinc oxide film. J. Appl. Phys. 80 (1996) 1063-1073.

[4] M. Krunks, E. Mellikov, Zinc oxide thin films by spray pyrolysis method, Thin Solid Films 270 (1995) 33-36.

[5] S. Fujihara, C. sasaki, T. Kimura, Crystallization behavior and origin of c-axis orientation in sol-gel derived ZnO:Li thin films on glass substrates, Appl. Surf. Sci. 180 (2001) 341- 350.

[6] F. Paraguay D, M. Miki-Yoshida, J. Morales, J. Solis, W. Estrada L, Influence of Al, In, Cu, Fe and Sn dopants on the response of thin film ZnO gas sensor to ethanol vapour, Thin Solid Films, 373 (2000) 137-140.

[7] P.P.Sahay, R. K. Nath, Al- doped Zinc oxide thin films for liquid petroleum gas (LPG) sensors, Sensors and Actuators B, article in press.

[8] T. Minami, H. Sato, H. Nanto, S. Takata, Group III impurity doped zinc oxide thin films prepared by RF magnetron sputtering. Jpn. J. Appl Phys. (Part2) 24 (1985) l781- l784.

[9] P.P.Sahay, S.Tiwari, and R.K.nath; Optical and electrical studies on spray deposited ZnO thin films. Cryst. Res. Technol. 42, No. 7, 723-729 (2007)

[10] P.P.Sahay, Zinc oxide thin film gas sensor for detection of acetone; Journal of Materials Science 40 (2005) 4383-4385.